

Lifetime Measurements of the Neutron-Rich $N = 30$ Isotones ^{50}Ca and ^{51}Sc : Orbital Dependence of Effective Charges in the fp Shell

J. J. Valiente-Dobón,^{1,*} D. Mengoni,² A. Gadea,^{1,3} E. Farnea,⁴ S. M. Lenzi,² S. Lunardi,² A. Dewald,⁵ Th. Pissulla,⁵ S. Szilner,⁶ R. Broda,⁷ F. Recchia,¹ A. Algora,^{3,8} L. Angus,⁹ D. Bazzacco,⁴ G. Benzoni,¹⁰ P. G. Bizzeti,¹¹ A. M. Bizzeti-Sona,¹¹ P. Boutachkov,¹² L. Corradi,¹ F. Crespi,¹³ G. de Angelis,¹ E. Fioretto,¹ A. Görgen,¹⁴ M. Gorska,¹² A. Gottardo,¹ E. Grodner,¹ B. Guiot,¹ A. Howard,¹⁵ W. Królas,⁷ S. Leoni,¹³ P. Mason,¹ R. Menegazzo,⁴ D. Montanari,¹³ G. Montagnoli,² D. R. Napoli,¹ A. Obertelli,¹⁴ T. Pawłat,⁷ G. Pollarolo,¹⁶ B. Rubio,³ E. Şahin,¹ F. Scarlassara,² R. Silvestri,¹ A. M. Stefanini,¹ J. F. Smith,⁹ D. Steppenbeck,¹⁵ C. A. Ur,⁴ P. T. Wady,⁹ J. Wrzesiński,⁷ E. Maglione,² and I. Hamamoto¹⁷

¹*Istituto Nazionale di Fisica Nucleare, Laboratori Nazionali di Legnaro, Legnaro, Italy*

²*Dipartimento di Fisica dell'Università and INFN Sezione di Padova, Padova, Italy*

³*Instituto de Física Corpuscular, CSIC-Universidad de Valencia, Valencia, Spain*

⁴*Istituto Nazionale di Fisica Nucleare, Sezione di Padova, Padova, Italy*

⁵*Institut für Kernphysik der Universität zu Köln, Köln, Germany*

⁶*Ruđer Bošković Institute, Zagreb, Croatia*

⁷*Institute of Nuclear Physics, Polish Academy of Sciences, Cracow, Poland*

⁸*Institute of Nuclear Research of the Hungarian Academy of Sciences, Debrecen, Hungary*

⁹*School of Engineering and Science, University of Paisley, Paisley, Scotland, United Kingdom*

¹⁰*Istituto Nazionale di Fisica Nucleare, Sezione di Milano, Milano, Italy*

¹¹*Dipartimento di Fisica dell'Università and INFN Sezione di Firenze, Firenze, Italy*

¹²*Helmholtzzentrum für Schwerionenforschung (GSI), Darmstadt, Germany*

¹³*Dipartimento di Fisica dell'Università and INFN Sezione di Milano, Milano, Italy*

¹⁴*CEA Saclay, IRFU/Service de Physique Nucléaire, Gif-sur-Yvette, France*

¹⁵*Schuster Laboratory, University of Manchester, Manchester, United Kingdom*

¹⁶*Dipartimento di Fisica Teorica, Università di Torino, Via Pietro Giuria I, I-10125 Torino, Italy*

¹⁷*Department of Mathematical Physics, Lund Institute of Technology at University of Lund, Lund, Sweden*
(Received 2 December 2008; published 16 June 2009; corrected 23 July 2009)

The lifetimes of the first excited states of the $N = 30$ isotones ^{50}Ca and ^{51}Sc have been determined using the Recoil Distance Doppler Shift method in combination with the CLARA-PRISMA spectrometers. This is the first time such a method is applied to measure lifetimes of neutron-rich nuclei populated via a multinucleon transfer reaction. This extends the lifetime knowledge beyond the $f_{7/2}$ shell closure and allows us to derive the effective proton and neutron charges in the fp shell near the doubly magic nucleus ^{48}Ca , using large-scale, shell-model calculations. These results indicate an orbital dependence of the core polarization along the fp shell.

DOI: 10.1103/PhysRevLett.102.242502

PACS numbers: 27.40.+z, 21.10.Tg, 21.60.Cs, 23.20.-g

Nuclei are mesoscopic systems composed of fermions characterized, as other finite quantum-mechanical many-body systems, by a shell structure with the presence of gaps in the single-particle spectra. The filling of the nucleon orbitals up to the shell gaps give rise to the well-known magic numbers in nuclei near stability: doubly magic nuclei are those with a closed shell for both protons and neutrons. Nuclei with few valence particles around doubly magic nuclei are crucial for the understanding of nuclear structure and ideal for studying the effective nucleon-nucleon interaction through comparison with shell-model calculations [1]. In such calculations, the electric charges of valence particles outside the adopted doubly magic core are not those of the bare nucleons ($e_{\pi} = 1.0e$, $e_{\nu} = 0.0e$), but “effective” charges are used which account for the degrees of freedom not explicitly included in the calculations. The standard assumption of the shell model is that the effective charges to be used are constant within a major

oscillator shell. This is indeed expected from a simple model in Bohr and Mottelson [2], where they are estimated using the harmonic oscillator potential with separable quadrupole-quadrupole interaction of isoscalar (IS) and isovector (IV) character. However, any deviation from the harmonic oscillator potential or from the separable character of the interaction may produce a dependence of the effective charges on particle orbits and/or isospin within a major shell. In this respect, the recent experimental advances in the study of neutron-rich nuclei far from stability allow us now to address this question for the $N = 3$ oscillator shell which spans nuclei from $Z, N = 20$ to $Z, N = 40$ (fp shell).

The calcium isotopes, which correspond to the $Z = 20$ closed shell, manifest doubly magic character for the stable ^{40}Ca and ^{48}Ca . Whereas nuclei in the vicinity of ^{40}Ca are well studied up to quite high spins, the knowledge of nuclei with few valence nucleons with respect to ^{48}Ca is limited to

some low-lying states populated in β -decay and only recently some of their properties could be studied by using multinucleon transfer stable-beam reactions [3,4] or radioactive beams [5,6]. A theoretical description in terms of shell-model calculations, using the best effective interactions available, is able to reproduce the trend in excitation energy of these nuclei around ^{48}Ca , but fails to account for the measured reduced electromagnetic transition probabilities [$B(E2)$] of the neutron-rich Ti and Cr isotopes [7,8]. The effective charges commonly adopted in such shell-model calculations for the fp shell are $e_\pi = 1.5e$, $e_\nu = 0.5e$ [9]. Recently, these values have been questioned and new values $e_\pi = 1.15e$ and $e_\nu = 0.8e$, determined from lifetime measurements of highly excited states in neutron-deficient $N \approx Z$ mirror nuclei [10], have been suggested. With these new effective charges, the $B(E2)$ values in neutron-rich Ti and Cr isotopes around $N = 32$ are again not well reproduced [11], even if, in the case of the Ti isotopes, a staggering, much lower than in experiment, appears.

Neutron-rich nuclei of the fp shell such as ^{50}Ca and ^{51}Sc are expected to have a simple structure involving mainly two neutrons in the $p_{3/2}$ orbital outside the doubly magic nucleus ^{48}Ca very different from that of the states of $N \approx Z$ nuclei of Ref. [10], where the orbital involved is $f_{7/2}$. The study of these nuclei, now feasible by means of multinucleon transfer reactions [3], gives therefore the opportunity to investigate how the core polarization changes along the fp shell. In this Letter, we report on the first measurement of nuclear lifetimes in the picosecond range using the differential Recoil Distance Doppler Shift method (RDDS) developed for multinucleon transfer reactions [12] in combination with the CLARA [13] and PRISMA [14] spectrometers. The lifetimes of the first 2^+ and $11/2^-$ states of the neutron-rich $N = 30$ isotones ^{50}Ca and ^{51}Sc , respectively, have been determined. The $B(E2)$ values extracted are compared with large-scale shell-model calculations, and for the first time, the effective charges in the fp shell near ^{48}Ca are derived.

The nuclei ^{50}Ca and ^{51}Sc were populated as products of a multinucleon transfer reaction following the collision of a ^{48}Ca beam onto a ^{208}Pb target. The ^{48}Ca beam, at a bombarding energy of 310 MeV, was delivered by the LNL Tandem-ALPI accelerator complex. The beam intensity was limited to 1 pnA to avoid thermal stress of the plunger-target device. The procedure for stretching simultaneously the target and the degrader foils as well as the dedicated target holder have been developed at the Institute of Nuclear Physics at the University of Köln [15]. The target consisted of 1.0 mg/cm² of enriched ^{208}Pb evaporated onto a 1.0 mg/cm² Ta support to accomplish the stretching of the target. A thick 4 mg/cm² $^{\text{nat}}\text{Mg}$ foil used as an energy degrader of the recoiling ejectiles was positioned after the target. Different target-degrader distances, ranging from 30 μm to 2200 μm , were employed

during the experiment by using various metallic distance rings, whose thickness accuracy was better than 1.0 μm . In this experiment, CLARA consisted of 23 Compton suppressed Clover detectors. However, the detectors placed around 90° with respect to the CLARA-PRISMA symmetry axis could not be used to measure lifetimes since the Doppler shift of a γ ray emitted in flight is close to zero for these detectors. Therefore, the number of useful detectors were 12, with a total photopeak efficiency of the order of 1.2%. After passing through the Mg degrader, the projectilelike products were selected with the magnetic spectrometer PRISMA placed at the grazing angle $\theta_{\text{LAB}} = 49^\circ$. Even with such a thick degrader, located between the target and the entrance of the spectrometer, PRISMA preserved an excellent mass resolution. A schematic view of the experimental setup can be seen in Fig. 1 of Ref. [16]. The use of an energy degrader in combination with the RDDS method has been previously used in cases where the heavy ions emitting the γ rays were eventually detected, such as in fission fragments spectroscopy [17], fusion-evaporation reactions [18], and more recently in fast-beam fragmentation [19]. This technique, applied to multinucleon transfer reactions, allows us not only to measure lifetimes of excited states in neutron-rich nuclei, but also to partially control the direct feeding and the feeding from higher lying states because the use of a spectrometer like PRISMA implies the possible selection of ranges of excitation energy of the reaction products via an appropriate gate on the Total Kinetic Energy Loss (TKEL) [16].

Figure 1 shows, for different target-degrader distances, Doppler-corrected γ -ray spectra associated with ^{50}Ca and ^{51}Sc for selected energy regions including their respective $2^+ \rightarrow 0^+$ 1027-keV and $11/2^- \rightarrow 7/2^-$ 1065-keV transitions. The Doppler correction is performed on an event-by-event basis using the velocity obtained by the reconstruction of the recoil trajectories in PRISMA. Depending on whether the γ ray was emitted before or after the degrader, it experiences different Doppler shifts. Therefore, for each transition, the γ spectrum shows two peaks. The higher-energy one, E_{After} , which presents an energy resolution of 0.6%, corresponds to γ rays emitted after passing the degrader, with an average velocity of $\langle\beta_{\text{After}}\rangle \approx 8.0\%$. The lower-energy one, E_{Before} , corresponds to γ rays emitted before the degrader, with an average velocity of $\langle\beta_{\text{Before}}\rangle \approx 10.0\%$. The relative intensities of the peak areas as a function of the target-degrader distance determines the lifetime of the state of interest. A detailed discussion and realistic simulations of the experimental method can be found in Ref. [16]. Figure 2 shows the negative logarithm of the experimental ratio $R = \frac{I_{\text{After}}}{I_{\text{Before}} + I_{\text{After}}}$, where $I_{\text{After,Before}}$ is the peak area of the transitions emitted after and before the degrader, for the different target-degrader distances, as well as the lifetime fit for both the 2^+ and the $11/2^-$ states in ^{50}Ca and ^{51}Sc , respectively. The lifetime obtained for the 2^+ state in ^{50}Ca is $\tau = 96 \pm 3$ ps. Different gates in the

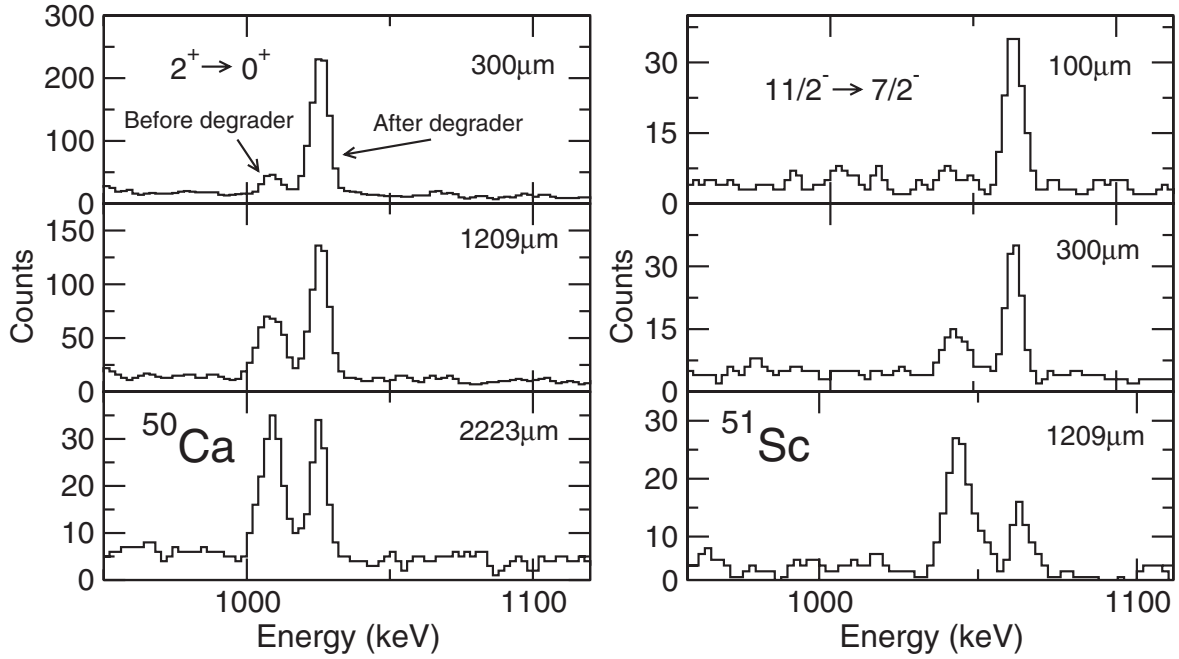


FIG. 1. Doppler-corrected γ -ray spectra showing the $2^+ \rightarrow 0^+$ 1027-keV and the $11/2^- \rightarrow 7/2^-$ 1065-keV transitions in ^{50}Ca and ^{51}Sc for different target-degrader distances. The higher-energy and lower-energy peaks correspond to the decays after and before the degrader, respectively.

TKEL value yielded always a lifetime compatible with this value, indicating that the states feeding the 2^+ level have much shorter lifetimes and hence do not significantly affect the measured lifetime. The lifetime obtained for the $11/2^-$ state in ^{51}Sc is $\tau = 28 \pm 7$ ps. The experimental errors take into account the statistical error and the velocity uncertainty. In the case of ^{51}Sc , a low-TKEL gate, which corresponds to low-excitation energies, was set in order to reduce the feeding from upper states that could bias the lifetime. The absence of such a feeding has been confirmed by the fact that after a low-TKEL gating, one does not observe any other γ peak, besides the $11/2^- \rightarrow 7/2^-$ 1065-keV transition in the ^{51}Sc γ spectrum. From the measured lifetimes, the reduced transition probabilities have been extracted, giving $B(E2 \downarrow) = 7.5 \pm 0.2 e^2 \text{fm}^4$ and $B(E2 \downarrow) = 21 \pm 5 e^2 \text{fm}^4$ for the $2^+ \rightarrow 0^+$ and the $11/2^- \rightarrow 7/2^-$ transitions in ^{50}Ca and ^{51}Sc , respectively (see Table I). The $B(E2)$ value obtained for the decay of the 2^+ state in ^{50}Ca is smaller than the corresponding value for the doubly magic nucleus ^{48}Ca $\{B(E2 \downarrow) = 19.4 \pm 2.1 e^2 \text{fm}^4$ [20]}. However, this fact is not surprising since the ratio of the $B(E2)$ values between ^{48}Ca and ^{50}Ca is 16/9, larger than unity, already when the simplest $p_{3/2} - f_{7/2}$ neutron configurations are assumed for the 2^+ states: $(f_{7/2}^{-1}, p_{3/2})_{2^+}$ in ^{48}Ca and $(p_{3/2}^2)_{2^+}$ in ^{50}Ca . Moreover, in the wave function of the 2^+ state of the doubly magic ^{48}Ca , an appreciable component of proton excitation from the sd to the fp shell is expected, compared with the case of ^{50}Ca .

The structure of ^{50}Ca constitutes a special case due to its simple configuration with two neutrons above the doubly

magic nucleus ^{48}Ca . In particular, the configuration of the 2^+ state can be built by aligning two neutrons in the $p_{3/2}$ orbital. Similarly, the $11/2^-$ state in ^{51}Sc corresponds to the further coupling of the ^{50}Ca 2^+ state to a proton in the $f_{7/2}$ orbital. In this ideal scenario, the present experiment allows us to determine, by comparing the experimental $B(E2)$ values with shell-model calculations, the neutron effective charge for the fp shell, but with the dominant contribution of the $p_{3/2}$ orbital. For this purpose,

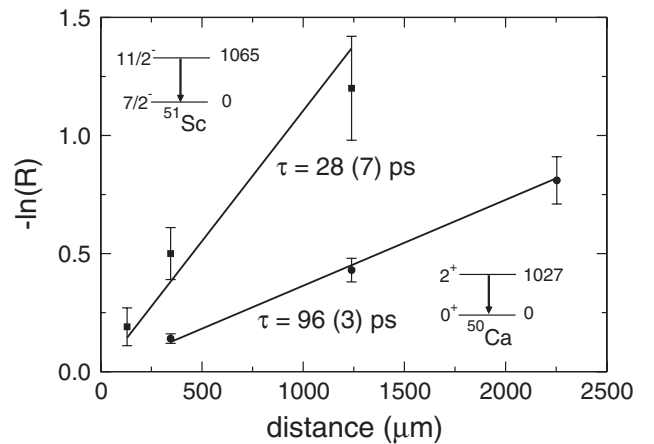


FIG. 2. Negative logarithm of the experimental ratio $R = \frac{I_{\text{After}}}{I_{\text{Before}} + I_{\text{After}}}$, where $I_{\text{After,Before}}$ is the peak area of the transitions emitted after and before the degrader, for the different target-degrader distances. It shows as well the fitted lifetime of the 2^+ and the $11/2^-$ states in ^{50}Ca and ^{51}Sc .

TABLE I. Comparison between the experimental and theoretical values of the transition energies and reduced electric quadrupole transition probabilities $B(E2 \downarrow)$ for ^{50}Ca and ^{51}Sc . The IS effective charges correspond to $e_\pi = 1.5e$ and $e_\nu = 0.5e$, while the IS + IV are $e_\pi = 1.15e$ and $e_\nu = 0.8e$.

	E_γ (keV)		$B(E2 \downarrow, J_i \rightarrow J_f)$ $e^2 \text{fm}^{4a}$	
	^{50}Ca	^{51}Sc	^{50}Ca	^{51}Sc
Exp.	1027	1065	7.5(2)	21(5)
KB3G (IS)	1060	1141	7.9	17.0
KB3G (IS + IV)			20.2	32.2
GXPFI1A (IS)	1187	1136	8.1	18.2
GXPFI1A (IS + IV)			20.7	33.6

^aFor ^{50}Ca : $J_i = 2^+$, $J_f = 0^+$ and ^{51}Sc : $J_i = 11/2^-$, $J_f = 7/2^-$

large-scale shell-model calculations, using the code ANTOINE [21,22], have been performed. The valence space was the fp shell with a core of ^{40}Ca . The KB3G [23] and GXPFI1A [24] effective interactions were used, without any restriction on the excitations within the fp shell. Both interactions reproduce well the excitation energy of the two states of interest (see Table I). The calculated wave functions, for both interactions, show a dominant ($\approx 86\%$) $\nu(f_{7/2}^8 p_{3/2}^2)$ configuration, for the ground state as well as for the 2^+ state in ^{50}Ca . The corresponding states in ^{51}Sc present a $\approx 74\%$ probability of the same neutron configuration coupled to the proton in the $f_{7/2}$ orbital. In the latter case, proton excitations to the upper orbits are very small, below 2%.

As stated above, to reproduce the experimental $B(E2)$ values, a necessary ingredient in the shell-model calculations is the proton and neutron effective charges, which depend on both the size of the inert core adopted and on the configuration space included in the calculations. According to Eq. (6–386) of Ref. [2], for a $N = Z$ core like ^{40}Ca , if only the isoscalar giant quadrupole resonance (GQR) excitation is considered, the effective charges for protons and neutrons are $e_\pi = 1.5e$ and $e_\nu = 0.5e$, respectively, the so called “standard” effective charges; if also the isovector GQR excitation is included, the effective charges for protons and neutrons are $e_\pi = 1.18e$ and $e_\nu = 0.82e$, respectively, which are very close to those obtained in Ref. [10] from the study of the $N \approx Z$ mirror nuclei ^{51}Fe - ^{51}Mn .

Table I shows the results of the large-scale shell-model calculations using both sets of effective charges. There is an excellent agreement, with the measured $B(E2)$ values, for the set ($e_\pi = 1.5e$ and $e_\nu = 0.5e$) in both nuclei and for both effective interactions, whereas there is a total disagreement for the set ($e_\pi = 1.15e$ and $e_\nu = 0.8e$). The neutron effective charge $e_\nu = 0.5e$ is determined very accurately, due to the precise lifetime measurement of ^{50}Ca and since the $B(E2)$ value is proportional to $(e_\nu)^2$. However, the proton effective charge has a larger ambiguity

due to the larger experimental error of the $B(E2)$ value in ^{51}Sc and to the fact that the proton contribution to the $B(E2)$ is small.

The choice of an harmonic oscillator potential when computing the transition probabilities within large shell-model calculations [21,22] might be not enough realistic, as the mean square radius, $\langle r^2 \rangle$, of the different orbitals in the fp model space is identical. Therefore, to further check the robustness of the comparison, the $B(E2)$ values have been calculated using a more realistic potential (Woods-Saxon), where the p orbits have a $\langle r^2 \rangle \approx 20\%$ larger than the f ones. The reduced transition probability calculated is slightly larger than the one obtained with the harmonic potential, calling for a neutron effective charge 15% smaller than the “standard” value ($e_\nu = 0.5e$). Consequently, it seems clear that the neutron effective charge for the neutron-rich $N = 30$ isotones is $e_\nu \approx 0.5e$. The nuclei studied in the present work have a higher neutron-to-proton ratio than the $N \approx Z$ nuclei of Ref. [10], and therefore the main configuration of the states for which lifetimes have been determined are quite different in the two cases. It involves mainly, two neutrons in the $\nu p_{3/2}^2$ orbital for the $N = 30$ isotones, while the configuration for the states in the $A = 51$ mirror nuclei is $f_{7/2}^{11}$. This seems to have clear consequences on the polarization of the core of ^{40}Ca and therefore on the effective charges.

An orbital dependence of the effective charges was indeed predicted from detailed theoretical investigations [25] in the shell-model framework. In particular, a considerable reduction for transitions involving p orbitals with respect to f orbitals was deduced, as confirmed by the present data. In addition, mean field studies on neutron-drip line nuclei suggested that the use of a fixed polarization charge for a given major shell in shell-model calculations might be questionable [26]. The fact that the neutron effective charge ($e_\nu = 0.5e$) deduced in this work from the $N = 30$ isotones is clearly smaller than that deduced in Ref. [10] is in agreement with both theoretical frameworks and clearly shows an orbital dependence of the core polarization within the fp shell.

In summary, the lifetimes of the first excited states of the $N = 30$ isotones ^{50}Ca and ^{51}Sc have been determined using a technique that combines the differential Recoil Distance Doppler Shift method with the CLARA-PRISMA setup. This opens important new perspectives for the measurement of lifetimes in neutron-rich nuclei, which were up to now inaccessible by standard experimental techniques. Effective proton and neutron charges, where both the f and p nucleons contribute to the $E2$ transitions, have been deduced after a detailed comparison with large-scale shell-model calculations. The values obtained by studying nuclei with large neutron-to-proton ratio within the fp shell, for excited states where the dominant contribution is due to $p_{3/2}$ neutrons, are compatible with the isoscalar effective charges ($e_\pi = 1.5e$ and $e_\nu = 0.5e$).

Though the value for the proton effective charge presents a larger ambiguity, the well-determined value $e_p = 0.5e$ is clearly different from the e_p value previously obtained for $f_{7/2}$ neutrons around $N \approx Z$. Therefore, this experimental result points to an orbital dependence of the effective charges in the fp shell, in contrast with the usual assumption that the effective charges should be constant within a major oscillator shell. *Ad pleniorem scientiam*, this question deserves further experimental and theoretical efforts.

We would like to thank A. Poves and A. Vitturi for fruitful and enlightening discussions. This work has been partially supported by the European Commission within the Sixth Framework Programme through I3-EURONS (Contract No. RII3-CT-2004-506065), the DFG (Germany under Contract No. DE1516/-1), and the Croatian MZOS 0098-1191005-2890 grant.

*valiente@lnl.infn.it

- [1] B. A. Brown, Prog. Part. Nucl. Phys. **47**, 517 (2001).
- [2] A. Bohr and B.R. Mottelson, *Nuclear Structure* (Benjamin Inc., New York, 1975), Vol II.
- [3] R. Broda *et al.*, J. Phys. G **32**, R151 (2006).
- [4] M. Rejmund *et al.*, Phys. Rev. C **76**, 021304(R) (2007).
- [5] L. A. Riley *et al.*, Phys. Rev. C **72**, 024311 (2005).
- [6] B. Bastin *et al.*, Phys. Rev. Lett. **99**, 022503 (2007).
- [7] D.-C. Dinca *et al.*, Phys. Rev. C **71**, 041302 (2005).
- [8] A. Bürger *et al.*, Phys. Lett. B **622**, 29 (2005).
- [9] E. Caurier, G. Martinez-Pinedo, F. Nowacki, A. Poves, and A. Zuker, Rev. Mod. Phys. **77**, 427 (2005).
- [10] R. du Rietz *et al.*, Phys. Rev. Lett. **93**, 222501 (2004).
- [11] A. Poves, F. Nowacki, and E. Caurier, Phys. Rev. C **72**, 047302 (2005).
- [12] A. Gadea *et al.*, Acta Phys. Pol. B **38**, 1311 (2007).
- [13] A. Gadea *et al.*, Eur. Phys. J. A **20**, 193 (2003).
- [14] A. Stefanini *et al.*, Nucl. Phys. A **701**, 217c (2002).
- [15] A. Dewald *et al.*, Nucl. Inst. and Methods, Sec. A (to be published).
- [16] D. Mengoni, Eur. Phys. J. A (to be published).
- [17] R. Krücken *et al.*, Phys. Rev. C **64**, 017305 (2001).
- [18] A. Dewald *et al.*, Phys. Rev. C **68**, 034314 (2003).
- [19] A. Dewald *et al.*, Phys. Rev. C **78**, 051302(R) (2008).
- [20] T. Hartmann, J. Enders, P. Mohr, K. Vogt, S. Volz, and A. Zilges, Phys. Rev. C **65**, 034301 (2002).
- [21] E. Caurier, Shell-model code ANTOINE, IRES, STRASBOURG (1989).
- [22] E. Caurier and F. Nowacki, Acta Phys. Pol. **30**, 705 (1999).
- [23] A. Poves, J. Sanchez-Solano, E. Caurier, and F. Nowacki, Nucl. Phys. A **694**, 157 (2001).
- [24] M. Honma, T. Otsuka, B. Brown, and T. Mizusaki, Eur. Phys. J. A **25**, 499 (2005).
- [25] P. Federman and L. Zamick, Phys. Rev. **177**, 1534 (1969).
- [26] I. Hamamoto, H. Sagawa, and X. Zhang, Nucl. Phys. A **626**, 669 (1997).